

Dynamic Contrast-Enhanced MR Imaging Predicts Local Control in Oropharyngeal or Hypopharyngeal Squamous Cell Carcinoma Treated with Chemoradiotherapy

Shu-Hang Ng^{1,2,3}, Chien-Yu Lin⁴, Sheng-Chieh Chan^{1,5}, Tzu-Chen Yen^{1,5}, Chun-Ta Liao⁶, Joseph Tung-Chieh Chang⁴, Sheung-Fat Ko², Hung-Ming Wang⁷, Shiang-Fu Huang⁶, Yu-Chun Lin^{2,3}, Jiun-Jie Wang^{3*}

1 Molecular Imaging Center, Chang Gung Memorial Hospital, Chang Gung University, Kueishan,, Taoyuan, Taiwan, **2** Department of Diagnostic Radiology, Chang Gung Memorial Hospital, Chang Gung University, Kueishan,, Taoyuan, Taiwan, **3** Department of Medical Imaging and Radiological Sciences, Chang Gung Memorial Hospital, Chang Gung University, Kueishan,, Taoyuan, Taiwan, **4** Department of Radiation Oncology, Chang Gung Memorial Hospital, Chang Gung University, Kueishan,, Taoyuan, Taiwan, **5** Department of Nuclear Medicine, Chang Gung Memorial Hospital, Chang Gung University, Kueishan,, Taoyuan, Taiwan, **6** Department of Otorhinolaryngology, Head and Neck Surgery, Chang Gung Memorial Hospital, Chang Gung University, Kueishan,, Taoyuan, Taiwan, **7** Department of Medical Oncology, Chang Gung Memorial Hospital, Chang Gung University, Kueishan,, Taoyuan, Taiwan

Abstract

The role of pretreatment dynamic contrast-enhanced perfusion MR imaging (DCE-PWI) and diffusion-weighted MR imaging (DWI) in predicting the treatment response of oropharyngeal or hypopharyngeal squamous cell carcinoma (OHSCC) to chemoradiation remains unclear. We prospectively investigated the ability of pharmacokinetic parameters derived from pretreatment DCE-PWI and DWI to predict the local control of OHSCC patients treated with chemoradiation. Between August, 2010 and March, 2012, patients with untreated OHSCC scheduled for chemoradiation were eligible for this prospective study. DCE-PWI and DWI were performed in addition to conventional MRI. The relationship of local control with the following clinical and imaging variables was analyzed: the hemoglobin level, T-stage, tumor location, gross tumor volume, maximum standardized uptake value, metabolic tumor volume and total lesion glycolysis on FDG PET/CT, transfer constant (K^{trans}), volume of blood plasma and volume of extracellular extravascular space on DCE-PWI, and apparent diffusion coefficient on DWI of the primary tumor. The patients were also divided into a local control group and a local failure group, and their clinical and imaging parameters were compared. There were 58 patients (29 with oropharynx squamous cell carcinoma [SCC] and 29 with hypopharynx SCC) with successful pretreatment DCE-PWI and DWI available for analysis. After a median follow-up of 18.2 months, 17 (29.3%) participants had local failure, whereas the remaining 41 patients achieved local control. Univariate analysis revealed that only the K^{trans} value was significantly associated with local control ($P = 0.03$). When the local control and local failure groups were compared, significant differences were observed in K^{trans} and the tumor location ($P = 0.01$ and $P = 0.04$, respectively). In the multivariable analysis, only K^{trans} was statistically significant ($P = 0.04$). Our results suggest that pretreatment K^{trans} may help predict the local control in OHSCC patients treated with chemoradiation.

Citation: Ng S-H, Lin C-Y, Chan S-C, Yen T-C, Liao C-T, et al. (2013) Dynamic Contrast-Enhanced MR Imaging Predicts Local Control in Oropharyngeal or Hypopharyngeal Squamous Cell Carcinoma Treated with Chemoradiotherapy. PLoS ONE 8(8): e72230. doi:10.1371/journal.pone.0072230

Editor: Zhuoli Zhang, Northwestern University Feinberg School of Medicine, United States of America

Received: April 9, 2013; **Accepted:** July 5, 2013; **Published:** August 7, 2013

Copyright: © 2013 Ng et al. This is an open-access article distributed under the terms of the Creative Commons Attribution License, which permits unrestricted use, distribution, and reproduction in any medium, provided the original author and source are credited.

Funding: we received grants from the National Science Council-Taiwan (99-2314-B-182A-095-MY3). The funders had no role in study design, data collection and analysis, decision to publish, or preparation of the manuscript.

Competing interests: The authors have declared that no competing interests exist.

* E-mail: jwang@mail.cgu.edu.tw

Introduction

Oropharyngeal and hypopharyngeal squamous cell carcinomas (OHSCC) are common malignant tumors of the head and neck that has long been considered as having similar risk factors and lymphatic drainage. However, human papillomavirus (HPV) is recently recognized to play a role in the pathogenesis of a subset of clinically and molecularly distinct head and neck squamous cell carcinomas (HNSCC), most

commonly located in the oropharynx. Patients with HPV-positive oropharyngeal SCC typically have lower age at onset, limited tobacco exposure, and more favorable prognosis compared with their HPV-negative counterparts [1,2]. Currently, an organ-preservation approach with chemoradiation has become an accepted treatment option for OHSCC [3]. However, such treatment mode is not always successful, and the reported local control rates were about 80% [4,5]. An early prediction of failure may allow for therapeutic modification,

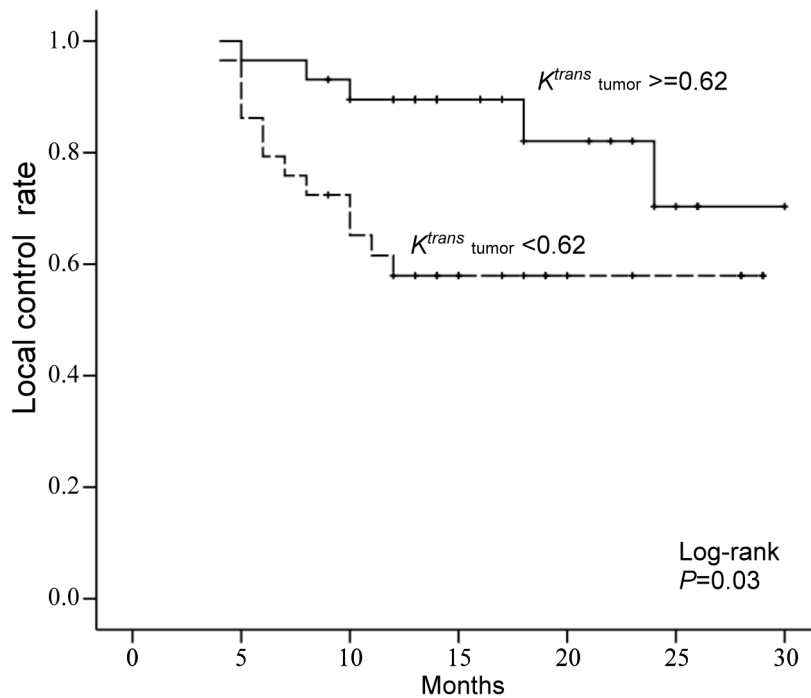


Figure 1. Kaplan-Meier analysis of local control rate stratified according to the median value of K^{trans} .

doi: 10.1371/journal.pone.0072230.g001

including the selection of suitable candidates for surgery in resectable OHSCC and the intensification of chemoradiation or the use of immunotherapy in unresectable cases [6,7]. Imaging biomarkers are being developed to identify tumors that are non-responsive to chemoradiation.

With the advance of MRI technology, diffusion-weighted MR imaging (DWI) and dynamic contrast-enhanced perfusion MR imaging (DCE-PWI) have become potential tools to evaluate the functional aspects of HNSCC. DWI is a quick MRI technique that can quantify the diffusion of water molecules in tissues using apparent diffusion coefficient (ADC). ADC has an inverse correlation with cell density [8,9], and the highly solid tumors (characterized by a lower ADC) may respond better to chemoradiation than tumors with a higher ADC. Because DWI takes only a few minutes to be acquired, it can be easily incorporated into routine head and neck MRI protocols. DCE-PWI is a functional MRI technique that based on sequential imaging obtained during the passage of a contrast agent through the tissue of interest. It is capable of probing the microvascular environment in the lesion, such as perfusion, the permeability of blood vessels and the volume of the extracellular space [10,11]. Since tumor oxygenation and tumor microvascular attenuation could be related to radiosensitivity [12], DCE-PWI is expected to help predict tumor responses to chemoradiation.

To date, only limited data are available regarding the use of pretreatment DCE-PWI or DWI to predict the chemoradiation response of HNSCC, and conflicting results have been

reported [4,7,13–18]. The hemoglobin (Hb) level [4,19,20], T-stage [21], tumor volume [4,5,22–24], as well as fluorodeoxyglucose-positron emission tomography (FDG-PET)/CT parameters, including the maximum standardized uptake value (SUV_{max}), metabolic tumor volume (MTV), and total lesion glycolysis (TLG) [25–27] have been reported to be correlated with local control, but reliable prediction of treatment response remains difficult. Therefore, we conducted a prospective study to determine whether the pretreatment DWI, DCE-PWI and the other reported potential factors can offer predictive power regarding to the local control of OHSCC in patients treated with definitive chemoradiation. To our knowledge, this is the first prospective study about the local control of OHSCC in patients undergoing chemoradiation evaluated with DWI and DCE-PWI, as well as FDG PET/CT.

Patients and Methods

Ethics Statement

The Institutional review board of the Chang Gung Memorial Hospital approved the study protocol (protocol no. 98-3582B) in September 2009. All participants gave written informed consent and the study followed the Declaration of Helsinki.

OHSCC Patients

The study protocol was approved by the local Institutional Review Board and written informed consent was obtained from all participants. Patients with newly diagnosed OHSCC

Table 1. Baseline characteristics of OHSCC patients (n = 58).

Characteristic	
Age (years)	
median	48.5
range	34-78
Sex (n (%) of patients)	
Male	54 (93.1)
Female	4 (6.9)
Hb value (g/dL)	
median	14.4
range	6.1-18.3
Tumor site (n (%) of patients)	
Hypopharynx	29 (50)
Oropharynx	29 (50)
Tumor volume (cm³)	
mean	35.84
range	1.9-144
T stage (n (%) of patients)	
1	4 (6.9)
2	11 (19)
3	6 (10.3)
4	37 (63.8)
N stage (n (%) of patients)	
0	10 (17.2)
1	4 (6.9)
2	33 (56.9)
3	11 (19)
Overall stage (n (%) of patients)	
II	3 (5.2)
III	3 (5.2)
IVA	38 (65.5)
IVB	14 (24.1)

scheduled for chemoradiation with curative intent were eligible for this prospective study. The study subjects underwent a thorough pretreatment evaluation, including MRI and ¹⁸F-FDG PET/CT. The exclusion criteria included the presence of a previous head or neck malignant tumor, a second malignant tumor or distant metastases, renal failure, or other contraindications for MRI. All of the patients were treated with intensity-modulated radiotherapy with a 6-MV X-ray at 2 Grays (Gy) per fraction, with five fractions per week. The radiotherapy dose was 46-50 Gy for all subclinical risk areas, including the neck lymphatics, and 72 Gy for primary tumor and grossly involved nodal disease. Concurrent chemotherapy consisted of cisplatin 50mg/m² on day 1, oral tegafur 800 mg/day plus leucovorin 60 mg/day from day 1 to day 14. It was repeated every two weeks through the radiotherapy course [28].

Following treatment, the patients underwent a routine follow-up clinical examination that included a physical examination and fiberoptic pharyngoscopy every 1 to 3 months. A follow-up MRI was performed 3 months after the treatment was completed, and additional MRI or CT was performed every 6 months thereafter or on clinical deterioration. Endoscopic biopsy, ultrasonographic guided fine needle aspiration, or CT-

guided biopsy was performed for any suspicious residual/recurrent tumors, if possible. If biopsy of the lesion of interest was not feasible or yielded a negative result, close clinical and imaging follow-up was pursued. Those patients without pathologically proven recurrence were followed up for at least 12 months after treatment or until death.

MRI with DWI and DCE-PWI

The MR imaging study was performed using a 3 Tesla MR scanner (Magnetom Trio with TIM, Siemens, Erlangen, Germany). Conventional MRI of the head and neck region was obtained in the axial and coronal projections with T2-weighted turbo spin echo (TSE) sequence with fat saturation plus T1-weighted TSE sequence, as well as with postcontrast fat-saturated T1-weighted TSE sequence.

The DWI was acquired using a single shot spin-echo echo-planar imaging with modified Stejskal-Tanner diffusion gradient pulsing scheme. Motion-probing gradients with a b-value of 800 s/mm² were applied along three orthogonal directions. The imaging slice and coverage were identical to the T1 and T2 weighted images. The repetition time (TR) and echo time (TE) were 8,200 ms and 84 ms, respectively.

DCE- PWI was acquired by using a 3D T1-weighted spoiled gradient-echo sequence with the following parameters: TR/TE = 3.5/1.13 ms, 230×230-mm field of view, 108×128 matrix, 5-mm section thickness, and 16 transverse sections in the volume. A spatial saturation slab was implanted inferior to the acquired region to minimize the inflow effect from the carotid arteries. Before the administration of the contrast agent, the baseline longitudinal relaxation time (T₁₀) values were calculated from images acquired with different flip angles (4°, 8°, 15°, and 25°). The dynamic series involved the use of the same sequence with a 15° flip angle. After four acquisitions of the dynamic baseline scanning, a standard dose (0.1 mmol/kg body weight) of gadopentetate dimeglumine (Gd-DTPA; Magnevist, Bayer-Schering, Burgess Hill, UK) was administered by a power injector through a cannula placed in the antecubital vein at a rate of 3 mL/s and immediately followed by a saline flush. A total of 80 volumes were acquired with a temporal resolution of 3.3 s.

Data Analysis

The ADC maps were reconstructed on a pixel-by-pixel basis using software integral to the MRI unit. The ADC was measured on ADC maps by drawing the region of interest (ROI) on the primary tumor at the level of its largest diameter by a radiologist with over 20 years of experience in head and neck imaging with the aid of the T2-weighted MR images and the T1-weighted post-contrast MR images. Visually large cystic or necrotic areas were avoided.

For DCE-PWI analysis, all of the data were processed in MATLAB 7.0 (The Mathworks, Natick, MA, USA). The signal intensities of the DCE-PWI data were converted from the contrast agent concentration by solving the nonlinear relationship between the signal intensity and the contrast agent concentration [29]. The extended Kety model [11] was adopted for the pharmacokinetic analysis in a voxel-wise manner. The arterial input function was extracted using the blind source

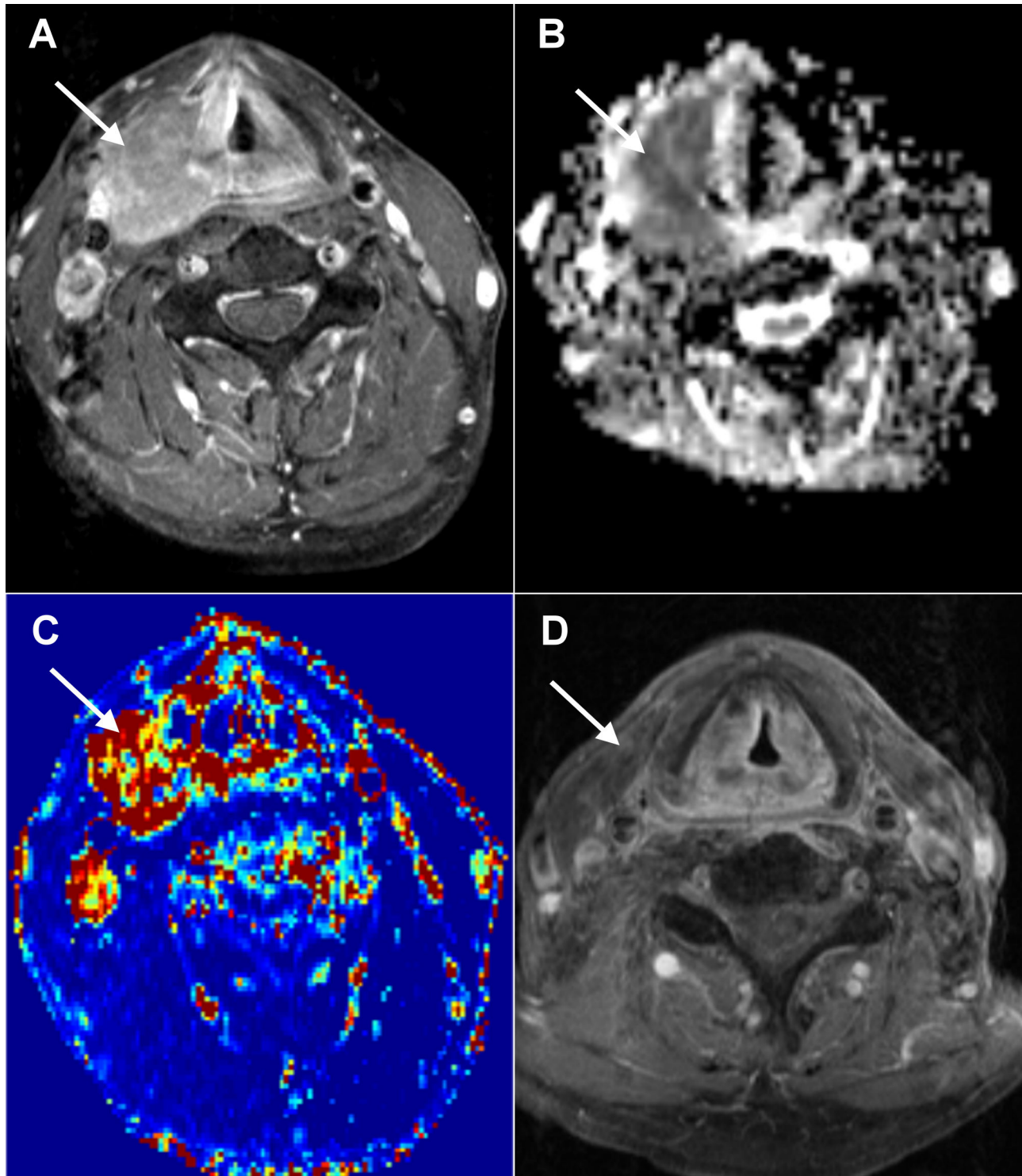


Figure 2. Local control in a 52-year-old man with hypopharyngeal SCC after chemoradiation. A. A pretreatment axial-enhanced MRI shows the right hypopharynx tumor (arrow). B. The corresponding PWI map shows the tumor with a K^{trans} value of 0.614 min^{-1} . C. The corresponding ADC map shows the tumor with an ADC value of $0.98 \times 10^{-3} \text{ mm}^2/\text{s}$. D. Post-treatment axial-enhanced MRI shows the regression of the right hypopharynx tumor. A 18-month clinical and imaging follow-up did not disclose any tumor growth.

doi: 10.1371/journal.pone.0072230.g002

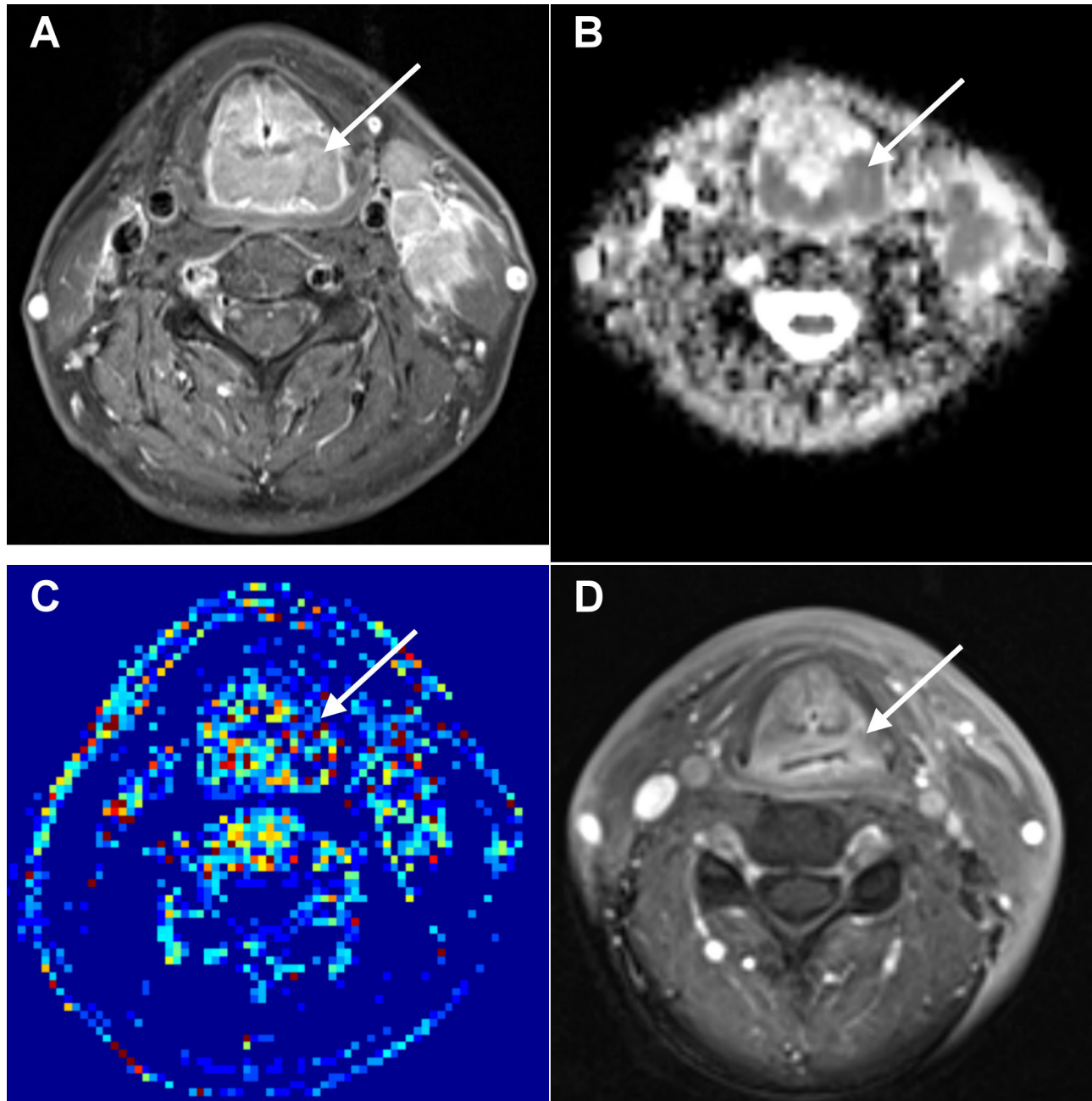


Figure 3. Local failure in a 61-year-old man with oropharyngeal SCC after chemoradiation. A. A pretreatment axial-enhanced MRI shows the oropharynx tumor (arrow). B. The corresponding PWI map shows the tumor with a K^{trans} value of 0.336 min^{-1} . C. The corresponding ADC map shows the tumor with an ADC value of $0.76 \times 10^{-3} \text{ mm}^2/\text{s}$. D. Post-treatment axial-enhanced MRI shows a residual left oropharynx tumor (arrow) which was proven by endoscopic biopsy.

doi: 10.1371/journal.pone.0072230.g003

separation algorithm [30], in which the extracted arterial voxel was located on the adjacent carotid artery of each patient. ROIs were manually drawn in the primary tumor on DCE MR images by the radiologist in a manner similar to that described for the DWI analysis. The following pharmacokinetic parameters were obtained: the volume transfer rate constant (K^{trans}), volume fraction of the extravascular extracellular space

(V_e), plasma volume (V_p), and redistribution rate constant (K_{ep}) which equals the ratio of K^{trans} to V_e .

The T-stage was recorded according to the 2010 cancer staging system revised by the American Joint Committee on Cancer. The gross tumor volume (GTV) of the primary tumor was calculated with a CT-based three-dimensional radiation treatment planning system. The SUV and the MTV of the

Table 2. Relationship between local failure and the variables.

	n	2-year control	P-value*	Hazard Ratio
Hb (g/dl)				
<12	12	50.0%	0.71	
> = 12	46	66.0%		
Tumor site				
Hypopharynx	29	53.5%	0.07	
Oropharynx	29	81.8%		
T stage				
T1-T2	15	75.0%	0.28	
T3-T4	43	59.5%		
GTV (cm³)				
<24.9	29	72.7%	0.25	
> = 24.9	29	51.5%		
SUV				
<15.31	28	78.2%	0.06	
> = 15.31	29	49.0%		
MTV(cm³)				
<23.28	28	74.9%	0.20	
> = 23.28	29	54.9%		
TLG				
<121.86	28	75.4%	0.18	
> = 121.86	29	51.5%		
K^{trans} (min⁻¹)				
<0.62	29	57.9%	0.03	0.34
> = 0.62	29	70.3%		
V_p × 10³				
<0.01	33	66.1%	0.47	
> = 0.01	25	59.7%		
V_e				
<0.2	29	60.9%	0.14	
> = 0.2	29	68.2%		
K_{ep}(min⁻¹)				
<2.63	29	61.1%	0.29	
> = 2.63	29	65.4%		
ADC(×10⁻³mm²/s)				
<0.96	27	64.8%	0.51	
> = 0.96	31	63.8%		

Abbreviations: GTV = Gross tumor volume; SUV = Standardized uptake value; MTV = Metabolic tumor volume; TLG = Total lesion glycolysis; ADC = Apparent diffusion coefficient*Log Rank test

primary tumor were measured from attenuation-corrected FDG PET images using the PMOD software (PMOD Technologies Ltd, Zurich, Switzerland). The boundaries were drawn large enough to include the primary tumor. An SUV threshold of 2.5 was used to delineate the MTV [31,32]. The contour around the target lesion inside the boundaries was automatically produced and the voxels presenting SUV intensity > 2.5 within the contouring margin were incorporated to define MTV. The SUV, MTV, and TLG of the lesion were automatically demonstrated by the software. The TLG was calculated as the product of the lesion mean SUV and the MTV.

Outcome Determination and Statistical Analysis

Local control was measured from the first day of treatment to the time of local failure or the last follow-up. Local failure was determined by histological confirmation (biopsy or surgical resection) or by a serial increase in lesion size on the follow-up imaging for at least 1 year. We used logistic regression analyses to analyze the relationship between the 2-year local control and the following baseline variables: the pretreatment Hb level, T-stage, tumor location, GTV of the primary tumor, SUV_{max}, MTV, and TLG on FDG-PET/CT, ADC on DWI, and K^{trans}, V_e, V_p and K_{ep} on DCE-PWI. We used the median values of the variables as the cutoff levels for the analysis [4,25]. The local control rates were plotted using the Kaplan-Meier method and compared using the log-rank test. OHSCC patients were also divided into a local control and a local failure group. The same variables mentioned above were compared between these two groups using an independent Student's *t*-test or the Pearson's chi-square test. For all the analyses, *P* values < 0.05 (two-tailed) were considered statistically significant. The variables showing significant differences were subjected to multivariable logistic regression analysis. A receiver operating characteristic (ROC) curve analysis was then performed to determine the value that best predicted local failure. All statistical analyses were performed using SPSS software version 13.0 (SPSS Inc., Chicago, IL, USA).

Results

Between August, 2010 and March, 2012, a total of 78 OHSCC patients underwent pretreatment DWI and DCE-PWI. Twenty patients were excluded from the analysis, 7 of whom had small or unevaluable (too necrotic) lesions, 9 had considerable artifact on DWI or PWI, and 4 were dead before the definite diagnosis of recurrence could be determined. Therefore, 58 patients were available for the analysis (29 oropharynx, 29 hypopharynx; 4 females and 54 males; median age, 48.5 ± 9.7 years). The patient characteristics are shown in Table 1. The pretreatment K^{trans} of the primary lesion ranged from 0.22 to 1.43 min⁻¹ (median, 0.62 min⁻¹), V_e ranged from 0.03 to 0.83 (median, 0.20), and V_p ranged from 0.001 to 0.94 (median, 0.01). The ADC of the primary lesion ranged from 0.67 to 1.59 × 10⁻³ mm²/s (median, 0.96 × 10⁻³ mm²/s). After chemoradiation, the response rates in our sample of 58 patients were as follows: complete response (*n* = 46; 79.3%), partial response (*n* = 10; 17.2%), and stationary disease (*n* = 2; 3.4%). Univariate logistic analysis showed that tumor site (*P* = 0.018), K^{trans} (*P* = 0.001), and V_e (*P* = 0.028) were significantly associated with complete response.

After a median follow-up time of 19.2 months (range, 9–32.3 months), 41 (70.7%) of the 58 patients achieved local control, whereas 17 (29.3%) patients had local failure. Local failure cases were confirmed by pathology for the presence of a viable tumor in 11 patients, or by disease progression in the remaining six. In univariate analysis, patients with a high pretreatment K^{trans} value had a significantly higher 2-year local control rate than those with a low K^{trans} value (*P* = 0.03, hazard ratio = 0.34, Figures 1-3). The other DCE-MRI parameters, including V_e, V_p and K_{ep}, showed no association with local

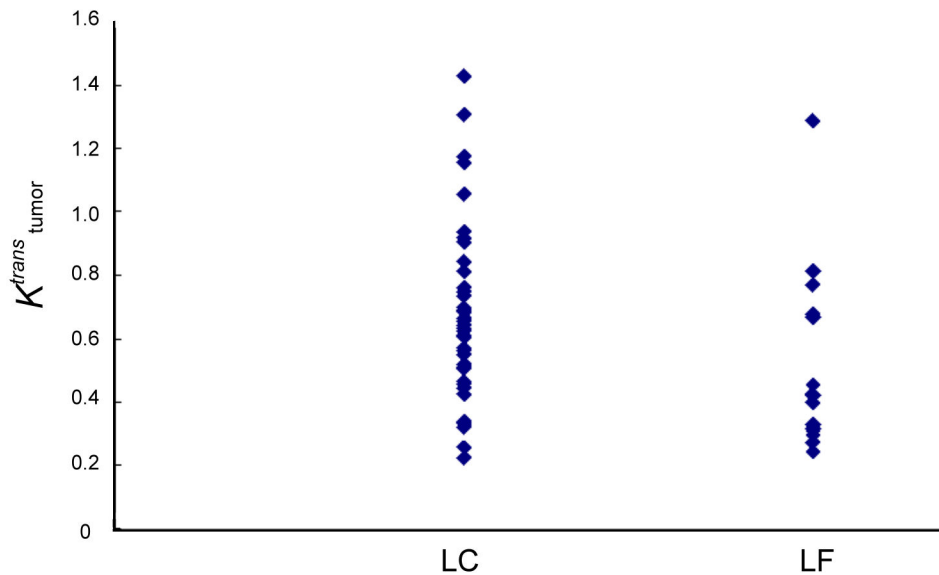


Figure 4. Scatterplots of K^{trans} in the local control (LC, $n=41$) and local failure (LF, $n=17$) groups.

doi: 10.1371/journal.pone.0072230.g004

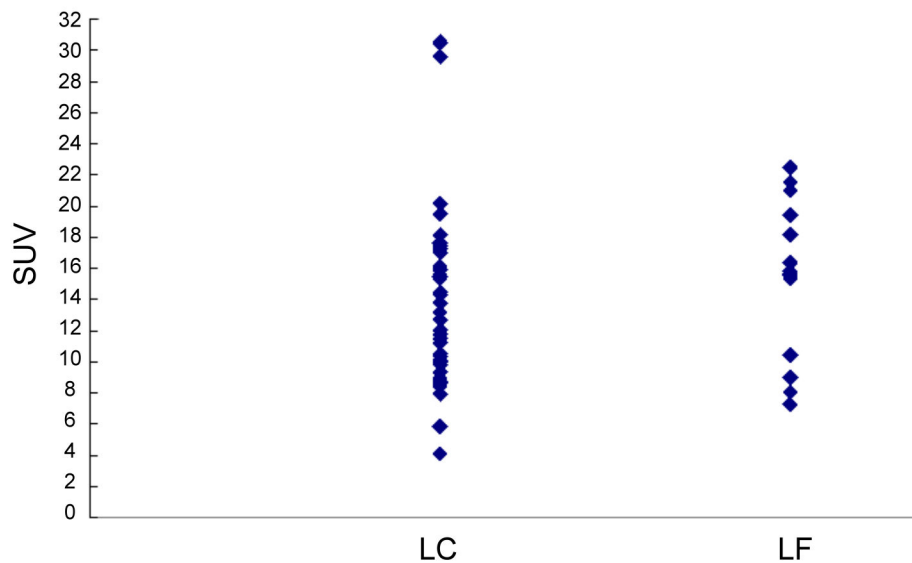


Figure 5. Scatterplots of SUV_{max} in the local control (LC, $n=41$) and local failure (LF, $n=17$) groups.

doi: 10.1371/journal.pone.0072230.g005

control. A tendency of a higher local control rate was found in patients with a low SUV_{max} as compared those with a high SUV_{max} ($P = 0.06$) and also in patients with oropharynx tumor as compared with those with hypopharyngeal tumor ($P = 0.07$). Patients with a low Hb level, high T-stage, high GTV, high MTV, or high TLG had lower 2-year local control rates than their counterparts, but the differences were not statistically significant. Patients with a high ADC level had similar local control rates as those with a low ADC value ($P = 0.51$; Table 2).

When the local control and local failure groups were compared, the average value of K^{trans} for the local control group was significantly higher than that of the local failure group (0.68 min^{-1} vs. 0.45 min^{-1} , $P = 0.001$, independent Student's t -test; Figure 4). The value of SUV_{max} for the local control group was also higher than that of the local failure group, but without statistical significance (Figure 5). The oropharynx tumors were associated with a significantly higher local control rate than the hypopharynx tumors (82.7% vs. 58.6% , $P = 0.04$, chi-square test). No significant difference was found for the ADC or the

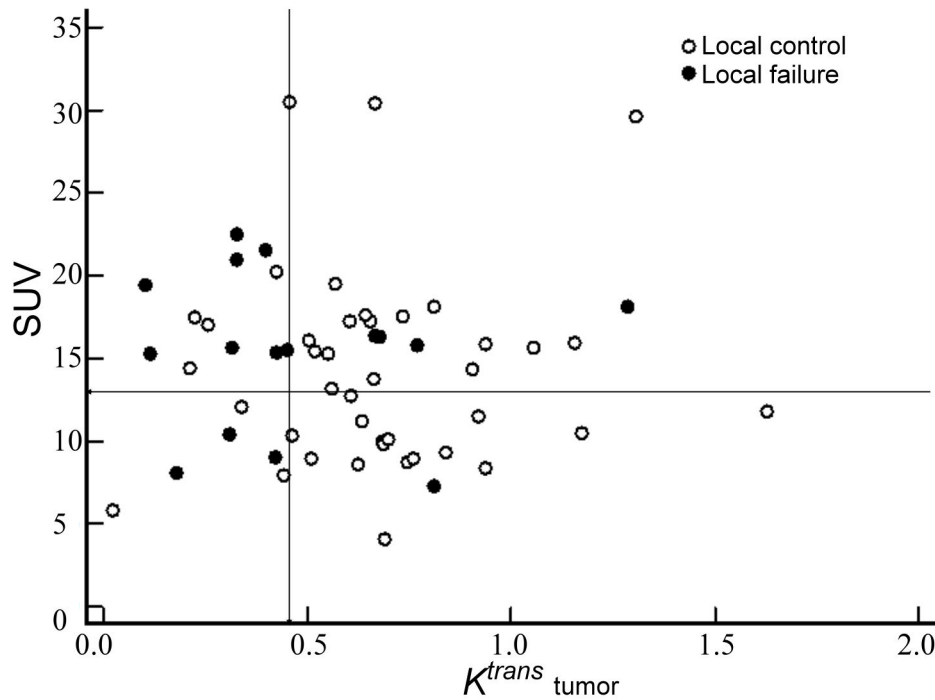


Figure 6. Scatterplots of the incidence of local failure with respect to the relationship between K^{trans} and SUV_{max} . The entire area of interest was divided into subsections (lines) using a cut-off of 0.45 min^{-1} for K^{trans} and a cut-off of 13.76 g/mL for SUV_{max} .
doi: 10.1371/journal.pone.0072230.g006

Table 3. Comparison of variables between the local control and local failure groups.

	Local control	Local failure	P value	Odds ratio
Hb (g/dL)	14±2.1	13.7±2.8	0.69*	
Tumor site				
Hypopharynx	17	12	0.04†	0.30
Oropharynx	24	5		
T stage				
T1-T2	12	3	0.51†	
T3-T4	29	14		
GTV (mL)	36±31.9	35.5±23.5	0.96*	
SUV (g/mL)	14.2±6	15.5±4.7	0.45*	
MTV (mL)	27.2±24.6	27.2±16.2	0.99*	
TLG (g)	168.4±173.8	171.3±116	0.95*	
K^{trans} (min^{-1})	0.7±0.3	0.5±0.3	0.01*	0.06
$V_p \times 10^3$	0.04±0.1	0.13±0.3	0.20*	
V_e	0.3±0.2	0.2±0.1	0.10*	
K_{ep} (min^{-1})	4.2±3.4	3.2±2.2	0.30*	
ADC ($\times 10^{-3} \text{mm}^2/\text{s}$)	1±0.2	1±0.1	0.77*	

Abbreviations: GTV = gross tumor volume; SUV = standardized uptake value; MTV = metabolic tumor volume; TLG = total lesion glycolysis; ADC = apparent diffusion coefficient*Independent Student's t-test †Pearson's chi-square test

other variables between both groups (Table 3). The multivariable logistic regression demonstrated that K^{trans} was the only significant predictor ($P = 0.04$) of local control. A K^{trans}

of 0.453 min^{-1} , determined by the ROC curve as a cutoff value for predicting local control, attained 70.6% sensitivity, 82.9% specificity, 63.1% positive predictive value and 87.2% negative predictive value. Because SUV_{max} value was marginally associated with local control ($P = 0.06$), we further assessed whether the SUV_{max} could improve the predictive value of K^{trans} for predicting local control. ROC analysis identified a SUV_{max} of 13.76 g/mL as the optimal cutoff for predicting local control. By combining the two variables, we were able to divide the patients into four distinct local control groups: Group 1, K^{trans} (min^{-1}) ≥ 0.45 and SUV (g/mL) < 13.76 ($n = 18$); K^{trans} (min^{-1}) ≥ 0.45 and SUV (g/mL) ≥ 13.76 ($n = 21$); K^{trans} (min^{-1}) < 0.45 and SUV (g/mL) < 13.76 ($n = 6$); K^{trans} (min^{-1}) < 0.45 and SUV (g/mL) ≥ 13.76 ($n = 13$). The local failure rates of Groups 1, 2, 3, and 4 were 5.6% (1/18), 19.0% (4/21), 50.0% (3/6), and 69.2% (9/13), respectively (Figure 6). The four groups were found to differ significantly in terms of 2-year local control rates (88.9%, 64.1%, 50.5%, and 30.8%; $P < 0.0001$, Figure 7)

Discussion

In this study, we evaluated the capability of pharmacokinetic parameters derived from pretreatment DCE-PWI and DWI in combination with other potential factors to predict the local control of cancer after chemoradiation in patients with OHSCC. This study showed that only the pretreatment K^{trans} of the primary tumor was significantly associated with local control rate, and K^{trans} was also significantly higher in the local control

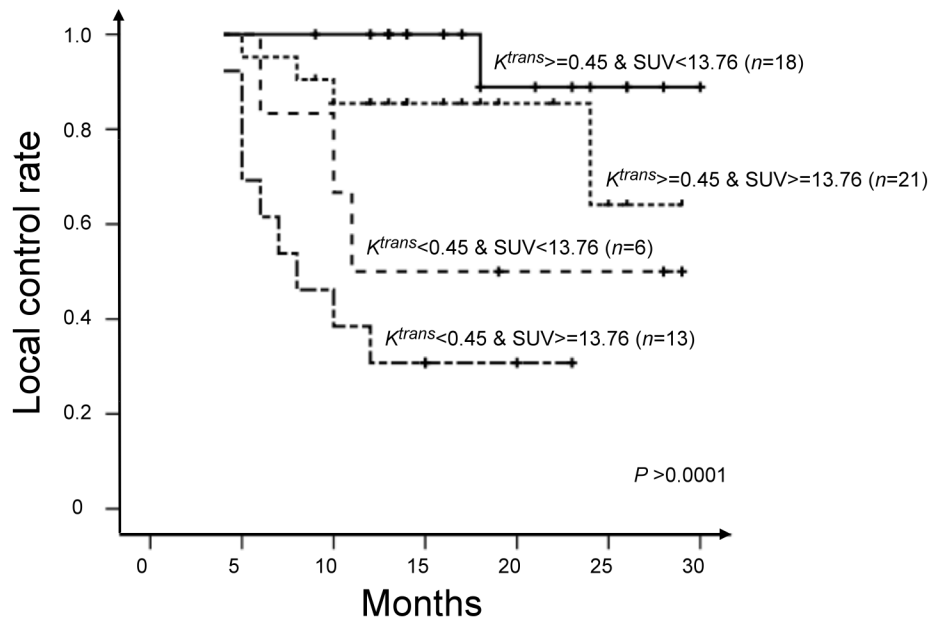


Figure 7. Subgroup analysis of local control rates according to different combinations of K^{trans} (cut-off = 0.45 min^{-1}) and SUV_{max} (cut-off = 13.76 g/mL).

doi: 10.1371/journal.pone.0072230.g007

group than in the local failure group. Since K^{trans} is the pharmacokinetic parameter of DCE-PWI that reflects tumor vascularity and permeability, it can influence the delivery of chemotherapy drugs as well as oxygen during radiotherapy. Accordingly, it is expected that tumors with a high K^{trans} would be associated with good treatment response. This explanation is consistent with the results of the present study. A better therapeutic response in lesions with high K^{trans} values has been documented in cervical cancer treated with radiotherapy [33] and colorectal cancer treated with chemoradiation [34]. However, another DCE-MRI study of colorectal liver metastases undergoing 5-fluorouracil treatment reported that the pretreatment K^{trans} did not predict the treatment response [35]. Therefore, the predictive value of K^{trans} for the treatment response may vary among different therapeutic strategies and tumor types. A few studies have investigated the capability of pretreatment DCE-PWI to predict the response of HNSCC to chemoradiation [7,16,18]. Ceo et al. [16] reported that an increase in blood volume in the primary tumor during radiotherapy was associated with local control while the pretreatment blood volume and blood flow were not significant predictors of the outcome. In a series of 33 patients with HNSCC, Kim et al. [7] demonstrated that the pretreatment K^{trans} of metastatic nodes of complete response patients was significantly higher than that observed for the partial response patients; no difference was found in V_e between the two patient groups. In a recent study of 15 HNSCC patients, Jansen et al.

[18] showed that the standard deviation of K^{trans} of metastatic nodes was a significant predictor of the short-term response, and again, V_e and K_{ep} were not of predictive value. Our study first documented that the K^{trans} of the primary tumor was the only DCE-PWI parameter associated with local control in OHSCC treated with chemoradiation, whereas V_e , V_p and K_{ep} did not function as predictors. A cutoff value of 0.4528 minutes^{-1} for K^{trans} attained 70.6% sensitivity and 82.9% specificity in predicting local control.

With regard to the usefulness of the pretreatment ADC for predicting the response to chemoradiation in HNSCC, one study demonstrated a significantly lower pretreatment ADC in lymph node metastases in complete responders than in partial responders [15], and two other reports found a significant correlation between the pretreatment ADC of a primary lesion and local treatment failure [14,17]. However, a conflicting result was reported in a larger study of 50 HNSCC patients [13]. The authors found that the pretreatment ADC of a primary tumor did not predict the chemoradiation response. The lack of an association between local control and the pretreatment ADC value of primary tumors in OHSCC patients observed in our study is consistent with the results of King et al. [13] and suggests that the primary tumor cellularity may not be a significant predictor of chemoradiation success.

SUV reflects the glucose metabolism of a tumor and is the widely used PET parameter. Pretreatment SUV_{max} of FDG PET has been reported to be an independent prognostic factor of

local control in HNSCC treated by radiotherapy or chemotherapy [25–27]. However, some other studies have reported the opposite result [31,36–40]; instead of SUV_{max} , MTV and TLG have been suggested to be adverse prognostic factors for local failure [31,38,39]. In the present study, we found that patients with high values of SUV_{max} , MTV or TLG had lower local control rates than those patients with lower values of these parameters, but only the SUV_{max} value was marginally significantly associated with 2-year local control ($P = 0.06$). Possible explanations for the discrepancies between the results of previous studies and the present study pertain to the variability in quantitative PET measurements that depend on technical parameters of data acquisition and processing, including the segmentation algorithm and the threshold chosen for these parameters. A larger-sized series with standardization of the quantification techniques of SUV, MTV, and TLG is needed to clarify their predictive values. Nevertheless, our study have showed that the combination of the low K^{trans} and high SUV_{max} of the primary tumor signified a subgroup of OPSCC patients at high risk of local failure. Consequently, these subjects are candidates for a more aggressive treatment approach.

Our findings agree with previous studies that patients with hypopharyngeal SCC had a worse outcome than patients with oropharyngeal SCC [24,32,39,41]. In this study, the tumor location (oropharynx versus hypopharynx) was weakly associated with the 2-year local control rate and showed slightly significant difference between the control and failure group, in which oropharyngeal SCC had better chemoradiation response than hypopharyngeal SCC. Therefore, oropharyngeal SCC showed a trend towards more local control than hypopharyngeal SCC, although the multivariable analysis revealed that the difference was not statistically significant. We suggest that more caution should be paid in chemoradiation selection and surveillance for hypopharyngeal SCC than for oropharyngeal SCC.

References

- Gillison ML, D'Souza G, Westra W, Sugar E, Xiao W et al. (2008) Distinct risk factor profiles for human papillomavirus type 16-positive and human papillomavirus type 16-negative head and neck cancers. *J Natl Cancer Inst* 100: 407-420. doi:10.1093/jnci/djn025. PubMed: 18334711.
- Ang KK, Harris J, Wheeler R, Weber R, Rosenthal DI et al. (2010) Human papillomavirus and survival of patients with oropharyngeal cancer. *N Engl J Med* 363: 24-35. doi:10.1056/NEJMoa0912217. PubMed: 20530316.
- Urba SG, Moon J, Giri PG, Adelstein DJ, Hanna E et al. (2005) Organ preservation for advanced resectable cancer of the base of tongue and hypopharynx: a Southwest Oncology Group Trial. *J Clin Oncol* 23: 88-95. PubMed: 15625363.
- Ohnishi K, Shioyama Y, Hatakenaka M, Nakamura K, Abe K et al. (2011) Prediction of local failures with a combination of pretreatment tumor volume and apparent diffusion coefficient in patients treated with definitive radiotherapy for hypopharyngeal or oropharyngeal squamous cell carcinoma. *J Radiat Res* 52: 522-530. doi:10.1269/jrr.10178. PubMed: 21905311.
- Studer G, Lütolf UM, El-Bassiouni M, Rousson V, Glanzmann C (2007) Volumetric staging (VS) is superior to TNM and AJCC staging in predicting outcome of head and neck cancer treated with IMRT. *Acta Oncol* 46: 386-394. doi:10.1080/02841860600815407. PubMed: 17450476.
- Worden FP, Kumar B, Lee JS, Wolf GT, Cordell KG et al. (2008) Chemoselection as a strategy for organ preservation in advanced oropharynx cancer: response and survival positively associated with HPV16 copy number. *J Clin Oncol* 26: 3138-3146. doi:10.1200/JCO.2007.12.7597. PubMed: 18474879.
- Kim S, Loevner LA, Quon H, Kilger A, Sherman E et al. (2010) Prediction of response to chemoradiation therapy in squamous cell carcinomas of the head and neck using dynamic contrast-enhanced MR imaging. *AJNR Am J Neuroradiol* 31: 262-268. doi:10.3174/ajnr.A1817. PubMed: 19797785.
- Hatakenaka M, Soeda H, Yabuuchi H, Matsuo Y, Kamitani T et al. (2008) Apparent diffusion coefficients of breast tumors: clinical application. *Magn Reson Med Sci* 7: 23-29. doi:10.2463/mrms.7.23. PubMed: 18460845.
- Gupta RK, Cloughesy TF, Sinha U, Garakian J, Lazareff J et al. (2000) Relationships between choline magnetic resonance spectroscopy, apparent diffusion coefficient and quantitative histopathology in human glioma. *J Neuro Oncol* 50: 215-226. doi:10.1023/A:1006431120031. PubMed: 11263501.
- Tofts PS (1997) Modeling tracer kinetics in dynamic Gd-DTPA MR imaging. *J Magn Reson Imaging* 7: 91-101. doi:10.1002/jmri.1880070113. PubMed: 9039598.
- Tofts PS, Brix G, Buckley DL, Evelhoch JL, Henderson E et al. (1999) Estimating kinetic parameters from dynamic contrast-enhanced T1-weighted MRI of a diffusible tracer: standardized quantities and symbols. *J Magn Reson Imaging* 10: 223-232. doi:10.1002/(SICI)1522-2586(199909)10:3. PubMed: 10508281.

Moreover, treatment response in HNSCC patients after radiotherapy has been reported to be significantly associated with the pretreatment hemoglobin levels and T stage [14,19,20,22,25–27], although there are some conflicting reports. Strongin et al [24] reported that the GTV was the best predictor of tumor control of HNSCC and found that the T stage was not a significant factor. Ohnishi et al [4] demonstrated that the GTV was more predictive of local control than the pretreatment Hb level or T-stage. However, according to Nathu et al. [22], the impact of the GTV was less pronounced than that of the T-stage on the local control of oropharyngeal SCC treated with radiotherapy. Moreover, variability in volume calculations of the GTV between observers is problematic. Our results support those studies that reported a lack of predictive power of the Hb level, T stage, and GTV, and suggest that these factors cannot be used as predictors for local control of OHSCC treated with chemoradiation.

Conclusions

Our results demonstrated that the pretreatment K^{trans} of the primary tumor was a significant predictor of local failure of OHSCC treated with chemoradiation, implying that tumor vascularity and permeability are more predictive of local control than tumor cellularity, metabolism, volume, and T-stage. The combination of K^{trans} with SUV_{max} , an imaging parameter that was marginally associated with local control rate in our study, improved the prognostic stratification of OHSCC patients who received chemoradiation with curative intent.

Author Contributions

Conceived and designed the experiments: SN TY JW CL. Performed the experiments: SN SC YL JW. Analyzed the data: SN CL SC SK SH. Contributed reagents/materials/analysis tools: SN TY CL TC HW. Wrote the manuscript: SN CL SC JW.

12. Kamijo T, Yokose T, Hasebe T, Yonou H, Sasaki S et al. (2000) Potential role of microvessel density in predicting radiosensitivity of T1 and T2 stage laryngeal squamous cell carcinoma treated with radiotherapy. *Clin Cancer Res* 6: 3159-3165. PubMed: 10955798.
13. King AD, Mo FK, Yu KH, Yeung DK, Zhou H et al. (2010) Squamous cell carcinoma of the head and neck: diffusion-weighted MR imaging for prediction and monitoring of treatment response. *Eur Radiol* 20: 2213-2220. doi:10.1007/s00330-010-1769-8. PubMed: 20309553.
14. Hatakenaka M, Nakamura K, Yabuuchi H, Shioyama Y, Matsuo Y et al. (2011) Pretreatment apparent diffusion coefficient of the primary lesion correlates with local failure in head-and-neck cancer treated with chemoradiotherapy or radiotherapy. *Int J Radiat Oncol Biol Phys* 81: 339-345. doi:10.1016/j.ijrobp.2010.05.051. PubMed: 20832179.
15. Kim S, Loevner L, Quon H, Sherman E, Weinstein G et al. (2009) Diffusion-weighted magnetic resonance imaging for predicting and detecting early response to chemoradiation therapy of squamous cell carcinomas of the head and neck. *Clin Cancer Res* 15: 986-994. doi: 10.1158/1078-0432.CCR-08-1287. PubMed: 19188170.
16. Cao Y, Popovtzer A, Li D, Chepeha DB, Moyer JS et al. (2008) Early prediction of outcome in advanced head-and-neck cancer based on tumor blood volume alterations during therapy: a prospective study. *Int J Radiat Oncol Biol Phys* 72: 1287-1290. doi:10.1016/j.ijrobp.2008.08.024. PubMed: 19028268.
17. Kato H, Kanematsu M, Tanaka O, Mizuta K, Aoki M et al. (2009) Head and neck squamous cell carcinoma: usefulness of diffusion-weighted MR imaging in the prediction of a neoadjuvant therapeutic effect. *Eur Radiol* 19: 103-109. doi:10.1007/s00330-008-1108-5. PubMed: 18641991.
18. Jansen JF, Schöder H, Lee NY, Stambuk HE, Wang Y et al. (2012) Tumor metabolism and perfusion in head and neck squamous cell carcinoma: pretreatment multimodality imaging with 1H magnetic resonance spectroscopy, dynamic contrast-enhanced MRI, and [18F]FDG-PET. *Int J Radiat Oncol Biol Phys* 82: 299-307. doi:10.1016/j.ijrobp.2010.11.022. PubMed: 21236594.
19. Lee WR, Berkey B, Marcial V, Fu KK, Cooper JS et al. (1998) Anemia is associated with decreased survival and increased locoregional failure in patients with locally advanced head and neck carcinoma: a secondary analysis of RTOG 85-27. *Int J Radiat Oncol Biol Phys* 42: 1069-1075. doi:10.1016/S0360-3016(98)00348-4. PubMed: 9869231.
20. Grant DG, Hussain A, Hurman D (1999) Pre-treatment anaemia alters outcome in early squamous cell carcinoma of the larynx treated by radical radiotherapy. *J Laryngol Otol* 113: 829-833. PubMed: 10664687.
21. Mendenhall WM, Morris CG, Amdur RJ, Hinerman RW, Mancuso AA (2003) Parameters that predict local control after definitive radiotherapy for squamous cell carcinoma of the head and neck. *Head Neck* 25: 535-542. doi:10.1002/hed.10253. PubMed: 12808656.
22. Nathu RM, Mancuso AA, Zhu TC, Mendenhall WM (2000) The impact of primary tumor volume on local control for oropharyngeal squamous cell carcinoma treated with radiotherapy. *Head Neck* 22: 1-5. doi: 10.1002/(SICI)1097-0347(200001)22:1. PubMed: 10585598.
23. Chen SW, Yang SN, Liang JA, Lin FJ, Tsai MH (2009) Prognostic impact of tumor volume in patients with stage III-IVA hypopharyngeal cancer without bulky lymph nodes treated with definitive concurrent chemoradiotherapy. *Head Neck* 31: 709-716. doi:10.1002/hed.21011. PubMed: 19260114.
24. Strongin A, Yovino S, Taylor R, Wolf J, Cullen K et al. (2012) Primary tumor volume is an important predictor of clinical outcomes among patients with locally advanced squamous cell cancer of the head and neck treated with definitive chemoradiotherapy. *Int J Radiat Oncol Biol Phys* 82: 1823-1830. doi:10.1016/j.ijrobp.2010.10.053. PubMed: 21549516.
25. Allal AS, Dulguerov P, Allaoua M, Haenggeli CA, El-Ghazi el A et al. (2002) Standardized uptake value of 2-[(18)F] fluoro-2-deoxy-D-glucose in predicting outcome in head and neck carcinomas treated by radiotherapy with or without chemotherapy. *J Clin Oncol* 20: 1398-1404. doi:10.1200/JCO.20.5.1398. PubMed: 11870185.
26. Allal AS, Slosman DO, Kibdani T, Allaoua M, Lehmann W et al. (2004) Prediction of outcome in head-and-neck cancer patients using the standardized uptake value of 2-[18F]fluoro-2-deoxy-D-glucose. *Int J Radiat Oncol Biol Phys* 59: 1295-1300. doi:10.1016/j.ijrobp.2003.12.039. PubMed: 15275712.
27. Torizuka T, Tanizaki Y, Kanno T, Futatsubashi M, Naitou K et al. (2009) Prognostic value of 18F-FDG PET in patients with head and neck squamous cell cancer. *AJR Am J Roentgenol* 192: W156-W160. doi: 10.2214/AJR.08.1429. PubMed: 19304675.
28. Wang HM, Wang CS, Chen JS, Chen IH, Liao CT et al. (2002) Cisplatin, tegafur, and leucovorin: a moderately effective and minimally toxic outpatient neoadjuvant chemotherapy for locally advanced squamous cell carcinoma of the head and neck. *Cancer* 94: 2989-2995. doi:10.1002/cncr.10570. PubMed: 12115388.
29. Schabel MC, Parker DL (2008) Uncertainty and bias in contrast concentration measurements using spoiled gradient echo pulse sequences. *Phys Med Biol* 53: 2345-2373. doi: 10.1088/0031-9155/53/9/010. PubMed: 18421121.
30. Lin YC, Chan TH, Chi CY, Ng SH, Liu HL et al. (2012) Blind estimation of the arterial input function in dynamic contrast-enhanced MRI using purity maximization. *Magn Reson Med*, 68: 1439-49. PubMed: 22383386.
31. Seol YM, Kwon BR, Song MK, Choi YJ, Shin HJ et al. (2010) Measurement of tumor volume by PET to evaluate prognosis in patients with head and neck cancer treated by chemo-radiation therapy. *Acta Oncol* 49: 201-208. doi:10.3109/02841860903440270. PubMed: 21000156.
32. Chan SC, Hsu CL, Yen TC, Ng SH, Liao CT et al. (2013) The role of 18F-FDG PET/CT metabolic tumour volume in predicting survival in patients with metastatic nasopharyngeal carcinoma. *Oral Oncol* 49: 71-78. doi:10.1016/j.oraloncology.2012.07.016. PubMed: 22959277.
33. Yamashita Y, Baba T, Baba Y, Nishimura R, Ikeda S et al. (2000) Dynamic contrast-enhanced MR imaging of uterine cervical cancer: pharmacokinetic analysis with histopathologic correlation and its importance in predicting the outcome of radiation therapy. *Radiology* 216: 803-809. PubMed: 10966715.
34. George ML, Dzik-Jurasz AS, Padhani AR, Brown G, Tait DM et al. (2001) Non-invasive methods of assessing angiogenesis and their value in predicting response to treatment in colorectal cancer. *Br J Surg* 88: 1628-1636. doi:10.1046/j.0007-1323.2001.01947.x. PubMed: 11736977.
35. van Laarhoven HW, Klomp DW, Rijpkema M, Kamm YL, Wagener DJ et al. (2007) Prediction of chemotherapeutic response of colorectal liver metastases with dynamic gadolinium-DTPA-enhanced MRI and localized 19F MRS pharmacokinetic studies of 5-fluorouracil. *NMR Biomed* 20: 128-140. doi:10.1002/nbm.1098. PubMed: 17006886.
36. Greven KM, Williams DW 3rd, McGuiert WF Sr., Harkness BA, D'Agostino RB Jr. et al. (2001) Serial positron emission tomography scans following radiation therapy of patients with head and neck cancer. *Head Neck* 23: 942-946. doi:10.1002/hed.1136. PubMed: 11754497.
37. Vernon MR, Maheshwari M, Schultz CJ, Michel MA, Wong SJ et al. (2008) Clinical outcomes of patients receiving integrated PET/CT-guided radiotherapy for head and neck carcinoma. *Int J Radiat Oncol Biol Phys* 70: 678-684. doi:10.1016/j.ijrobp.2007.10.044. PubMed: 18262086.
38. La TH, Filion EJ, Turnbull BB, Chu JN, Lee P et al. (2009) Metabolic tumor volume predicts for recurrence and death in head-and-neck cancer. *Int J Radiat Oncol Biol Phys* 74: 1335-1341. doi:10.1016/j.ijrobp.2008.10.060. PubMed: 19289263.
39. Lim R, Eaton A, Lee NY, Setton J, Ohri N et al. (2012) 18F-FDG PET/CT metabolic tumor volume and total lesion glycolysis predict outcome in oropharyngeal squamous cell carcinoma. *J Nucl Med* 53: 1506-1513. doi:10.2967/jnumed.111.101402. PubMed: 22895812.
40. Chung MK, Jeong HS, Park SG, Jang JY, Son YI et al. (2009) Metabolic tumor volume of [18F]-fluorodeoxyglucose positron emission tomography/computed tomography predicts short-term outcome to radiotherapy with or without chemotherapy in pharyngeal cancer. *Clin Cancer Res* 15: 5861-5868. doi:10.1158/1078-0432.CCR-08-3290. PubMed: 19737951.
41. Chang MF, Wang HM, Kang CJ, Huang SF, Lin CY et al. (2010) Treatment results for hypopharyngeal cancer by different treatment strategies and its secondary primary—an experience in Taiwan. *Radiol Oncol* 5: 91. doi:10.1186/1748-717X-5-91. PubMed: 20925962.